The Petrophysical Characteristics of the Sinjar Formation, Kirkuk Oil Field, Northeastern Iraq

Radhwan K. H. Alatroshe[1*] iD , **Ammar R. Algburi [2]** iD

[1] Department of Geology, College of Science, University of Mosul, Mosul, Iraq.
[2]Department of Petroleum Reservoir Engineering, College of Petroleum and Mining Engineering, University of Mosul, Mosul, Iraq.

ABSTRACT

The current research presents a petrophysical evaluation of the carbonate reservoir rocks of Sinjar Formation units (Paleocene-Early Eocene) in well (K-319), Kirkuk Oilfield, northeastern Iraq. The thickness of the formation is about 55 m, and it is divided into two units, the lower unit (23 m), which includes successive limestone and dolomitic limestone, and the upper unit (32 m), which includes dolomitic limestone beds. Thin sections, wireline logs (density, neutron, and gamma-ray), and modern programs have been used to study the accumulation and productivity of hydrocarbons in this oilfield through the study of reservoir properties including volume of shale, lithology, calculating and classifying of porosity, and reservoir partitioning, which is determined based on interpreted and analyzed data from logs. According to the petrophysical properties of the reservoir rocks, Sinjar Formation is divided into four porosity zones, zone (A) that demonstrates very good porosity (25-35%), zones (B and D) of intermediate to good porosity (10-25%), and zone (C) that exhibits poor porosity (5-12%) because of the high shale content, which hinders the fluid flow and reduces porosity. Thin sections are examined for porosity classification. There are two main porosity types in Sinjar Formation. The first type is interparticle porosity in its three classes, class (a) of grainstone facies, class (b) of packstone facies, and class (c) of mudstone facies. The second type is vuggy porosity of both types: separate vug pores and touching vug pores. The interparticle porosity is considered one of the most critical features affecting the transport of liquids and gases inside rocks.

الخصائص البتروفيزيائية لتكوين سنجار، حقل نفط كركوك، شمال شرقي العراق

رضوان خليل حيدر الاتروشي[1]* ، عمار رمضان الجبوري[2]

[1] قسم علوم الارض، كلية العلوم، جامعة الموصل، الموصل، العراق.

[2] قسم هندسة المكامن النفطية، كلية هندسة النفط والتعدين، جامعة الموصل، الموصل، العراق.

الملخص

يقدم البحث الحالي تقييماً بتروفيزيائياً لمكمن الصخور الكاربوناتية لوحدات تكوين سنجار (الباليوسين – الأيوسين المبكر) في البئر (K-319) في حقل كركوك النفطي، شمال شرقي العراق. يبلغ سمك التكوين حوالي 55 م، وينقسم إلى وحدتين، الوحدة السفلى وسمكها 23 م، والتي تتكون من تعاقب طبقات الحجر الجيري والحجر الجيري الدولوماتي، والوحدة العليا سمكها 32 م، والتي تتكون من طبقات من الحجر الجيري الدولوماتي. تم استخدام الشرائح الصخرية والمجسات الثلاثة (الكثافة والنيوترون وأشعة كاما) والبرامج الحديثة لدراسة تراكم وإنتاج الهيدروكاربونات في حقل كركوك. ومن خلال دراسة الخصائص المكمنية بما في ذلك حجم السجيل والصخارية وحساب وتصنيف المسامية، تم تقسيم الخزان المكمني لتكوين سنجار بناءً على البيانات المفسرة والمحللة من المجسات المدروسة. وفقا للخصائص البتروفيزيائية للصخور المكمنية، ينقسم تكوين سنجار إلى أربع أنطقة مسامية وهي، النطاق (A) الذي يظهر مسامية جيدة جدا (25–35%)، والنطاقان (B و D) اللذان يُظهران مسامية متوسطة إلى جيدة (10–25%)، والنطاق (C) الذي يُظهر مسامية ضعيفة (5–12%) بسبب المحتوى العالي من السجيل الذي يعيق تدفق السوائل ويقلل المسامية. تم فحص الشرائح الصخرية لتصنيف المسامية، وهناك نوعان رئيسيان من المسامية في تكوين سنجار، النوع الأول هو المسامية بين الحبيبات وبأصنافها الثلاثة، الصنف (a) الذي يمثل سحنة الحجر الجيري الحبيبي، والصنف (b) الذي يمثل سحنة الحجر الجيري المرصوص، والصنف (c) الذي يمثل سحنة الحجر الجيري الطيني. اما النوع الثاني فهو يمثل المسامية الفجوية بنوعيها: المسامية الفجوية المنفصلة والمسامية الفجوية المتلامسة. وتعتبر المسامية من النوع الاول من أهم العوامل المؤثرة على تدفق السوائل والغازات في الصخور.

Introduction

The Sinjar Formation (Paleocene-Early Eocene) was first known in Jabal Sinjar region, near the village of Mamissa in Nineveh Governorate, northwestern Iraq with a thickness of (176 m), which consists of fossiliferous limestone with strata of dolomitic limestone (Bellen *et al.,* 1959; Jassim and Goff, 2006). The Sinjar Formation in the type section consists of three distinct facies: coral reef (Algae facies), back reef (Miliolids), and fore-reef (Nummulites) indicating a lagoon environment (Al-Saddiki, 1968; Jassim and Goff, 2006).

The Tertiary reservoir is composed of several economically important main reservoirs in Iraq including the Sinjar Formation reservoir (Aqrawi *et al.,* 2010). The limestone beds of Sinjar Formation have a low volume of porosity, but due to grain dissolution, a wide range of molding and vuggy pores are resulted with the integration of fracturing, enhancing the porous connectivity and constructing fluid flow in the rock units (Garland *et al.,* 2010; Rashid *et al.,*

2017). However, fracturing enhances pore connectivity and creates extensive fracture permeability, ultimately improving fluid productivity in the rock units.

Based on facies analysis, an open shelf environment represents the Sinjar Formation in the Bazyan anticline, Sulaymaniyah region (Fadhil *et al.,* 2021). The carbonate sediment in the Sinjar Formation shows very good magnitudes of porosity with high secondary porosity in the Taq-Taq Oilfield (Hussein, 2021). The Sinjar Formation consists of the thick dolomitic limestone succession in Sulaymaniyah Governorate (Karim *et al.,* 2018). This research aims to evaluate the petrophysical properties and production potential of the Sinjar Formation reservoir in Kirkuk Oilfield.

Geological Setting

The Kirkuk Oilfield is considered one of the biggest fields in the world, and is located in northeastern Iraq. This field is characterized by a longitudinal box-shaped structure convex fold with a total length of (98 km), and a width of (3-4 km) approximately. The fold's edges exhibit two asymmetrical plunges with an axis extending northwest-southeast (Aqrawi *et al.,* 2010).

Kirkuk Oilfield is branched from the northwest to the southeast into three domes, Khurmala, Avanah, and Baba (Al-Sakini, 1992). The study well is located within the Avanah dome parallel to Kirkuk's northern and northwestern outskirts of coordinates (35° 45' 45.30" N) and (44° 1' 15.60" E) (North Oil Company, 1990) (Fig. 1).
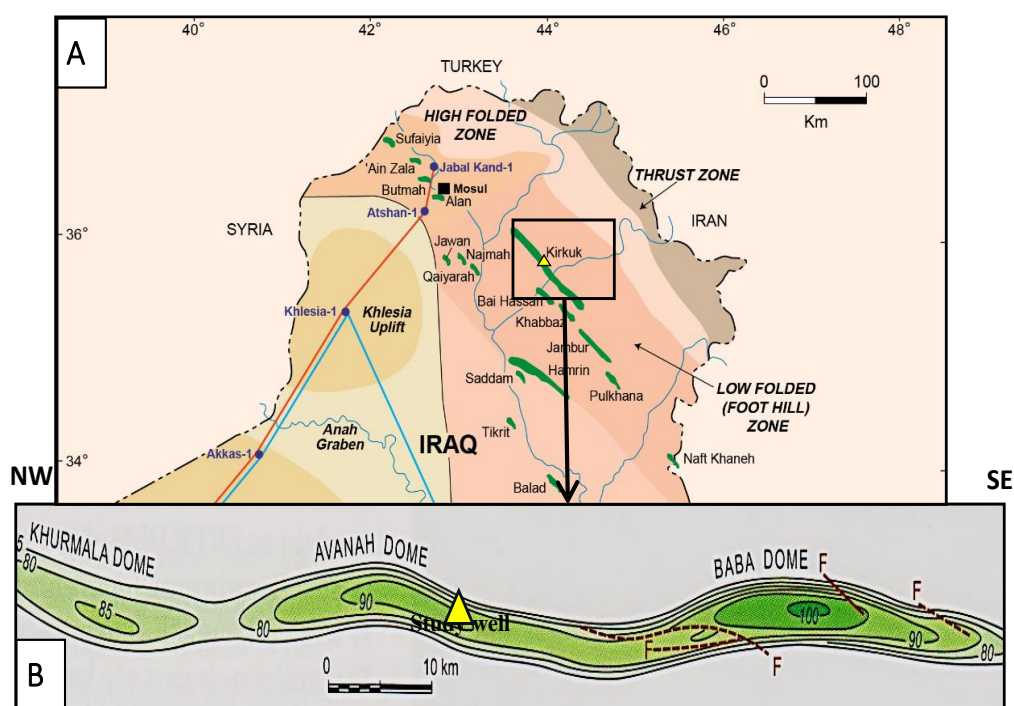

Fig.1. Map of petroleum fields in Iraq showing the location of the studied well. (A) Aqrawi (1998); (B) Aqrawi et al. (2010).

Tectonically, according to Fouad's (2015) divisions, the study well exists within the low folded zone (Fig. 2). These structures in the folded zone are characterized by symmetrical anticlines with carbonate rocks that offer various potential hydrocarbon reservoirs and oil productivity in northern Iraq (Aqrawi *et al.,* 2010; Fouad, 2015; Hussein *et al.,* 2018; Rashid *et al.,* 2020).
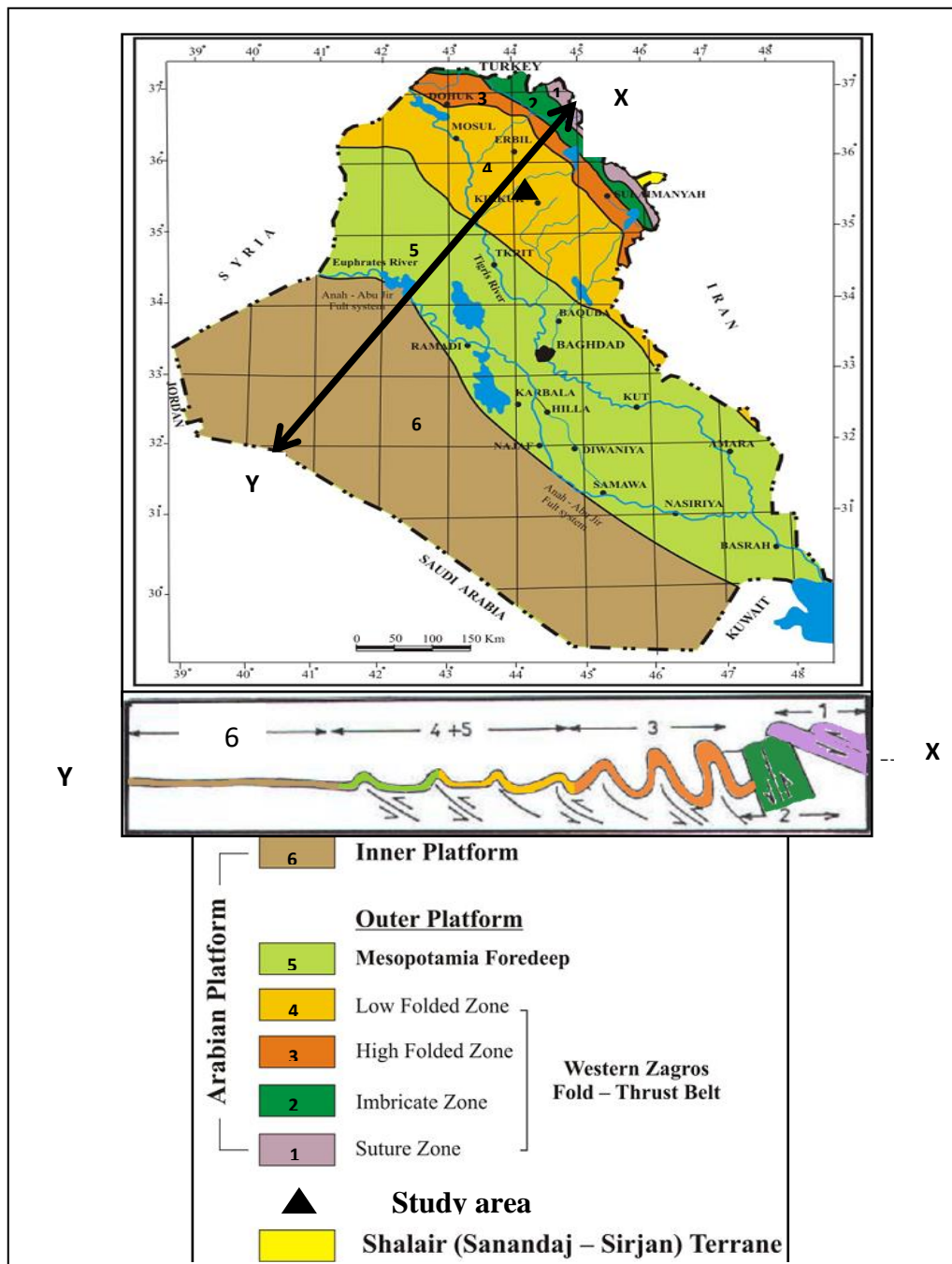
Fig. 2. Tectonic map of Iraq showing the research area (modified from Fouad, 2015).

Sinjar Formation has a thickness of about (55 m) and a depth range from (938 m) to (993 m) in well (K-319). This formation is branched into the lower unit (23 m), which includes limestone with a successive bed of dolomitic limestone, and the upper unit (32 m) is represented by dolomitic limestone. Sinjar Formation is located in the study well between the two conformable contacts, the upper contact with Khurmala Formation, and the lower contact with Kolosh Formation (Fig. 3).

Fig. 3. Lithology column of the Sinjar Formation.

Materials and Methods

According to the data recorded, two main categories of the methods are used in this study.

1- Data of well log

The data of electronic transcripts of the well logs (density, neutron, and gamma-ray) are gained from the North Oil Company in the Kirkuk Oilfield. These data are digitized within LAS file format for easy to handle using Neuralog (V-2010.11) software; then, Interactive Petrophysics software (V-3.6) to calculate porosity using a petrophysical analysis of logs data. Common mathematical equations and some standard schemes such as Schlumberger's have been applied to the current study of the logs.

2- Thin sections

A polarizing microscope is used to describe lithology in order to classify the formation's porosity depending on (20) thin sections prepared for this purpose. By this method, petrophysical properties can be better understood (Schlumberger, 1997; Rider and Kennedy, 2011).

Results and Discussion

The use of the following petrophysical parameters includes a gamma-ray (GR) index, the volume of the shale (V-Sh), lithology identification, calculating and classifying of porosity (φ) that are crucial in understanding the potential of a reservoir, and optimizing hydrocarbon exploration with production. These parameters are discussed below:

1- Gamma Ray (GR) Index

The GR record measures naturally occurring gamma radiation from the uranium, thorium, and potassium to characterize the rock or sediment in a borehole. Hydrocarbon-rich formations typically have lower gamma-ray readings compared to non-hydrocarbon-bearing formations. This is because the presence of organic materials in hydrocarbon rocks tends to emit less gamma radiation (Asquith and Krygowski, 2004).

In this study, GRlog is used to determine the index of gamma ray (IGR) by lowering an instrument into the drilled well and measuring the variation in gamma radiation with depth using the following equation (1) (Bassiouni, 1994).

$$I_{GR} = (GR_{log} - GR_{min}) / (GR_{max} - GR_{min}) \ldots\ldots (1)$$

where: I_{GR}= Gamma ray index value; GR_{log}= Gamma ray reading; GR_{min}= Minimum gamma ray index; GR_{max}= Maximum gamma ray index.

Shale baseline is determined where gamma ray logs record a maximum reading of (100) API (American Petroleum Institute unit); on the other hand, for clean sand line, the gamma reading is equal to (0.0) API, with the GR_{log} read from the log interval (Bhuyan and Passey, 1994).

This research uses a gamma-ray (GR) curve (Fig. 4) to identify shale volume in the studied field; this is important because a shale volume is frequently used to distinguish between the reservoir and non-reservoir rocks (Paul, 2010). Since the high concentration of radioactive materials is in shale, high gamma ray readings are recorded (Assaad, 2009).

2- Volume of shale (V_{Shale})

Based on the age of the Sinjar Formation, the Tertiary rocks equation is used to determine the shale volume (Equation 2) (Larionov, 1969). The calculation of gamma-ray values provides a representation of shale sequences about the depths of the Sinjar Formation distributed vertically within the formation from top to bottom (Fig. 4).

$$V_{Shale} = 0.083* [2^{(3.7*I_{GR})} - 1] \ldots\ldots\ldots\ldots..\ldots (2)$$

where: V_{Shale}= Volume of shale; I_{GR}= Index of gamma ray value.

Based on the shale volume ratio, the minimum gamma ray is 10 API at a depth of 985 m, which represents the gamma-ray reading for clean shale. On the other hand, the maximum gamma ray is 78 API at a depth of 973 m representing the gamma-ray reading for shale content (Ghorab *et al.,* 2008).

By comparing these GR values at different depths, valuable insights can be gained onto the characteristics of the shale sequences within the studied formation, which exhibits varying percentages of shale volume up to an average of (5%) (Fig. 4). As a result, the Sinjar Formation is clean-formation.
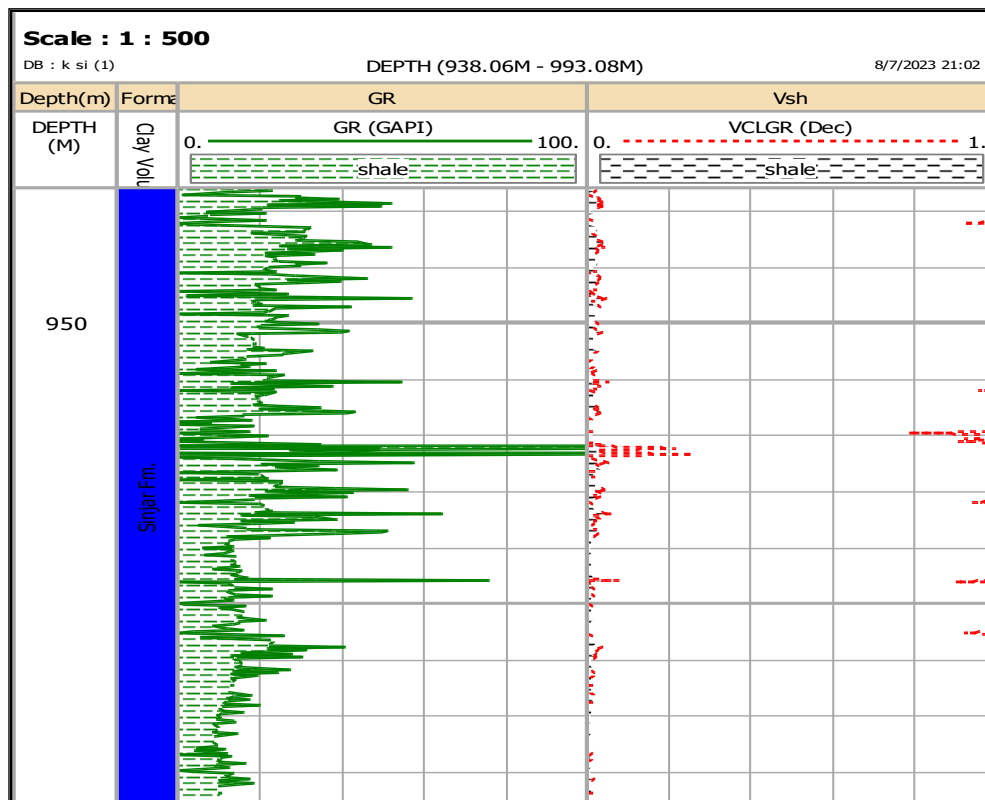

Fig. 4. The gamma ray log and shale volume ratio of the studied formation.

3- Lithology Identification

For carbonate formations such as the Sinjar Formation, the ideal method for determining lithology is to use a combination of both cross-plot neutron-density (N-D) logs (Burke *et al.,* 1969; Schlumberger, 1997; Rider and Kenedy, 2011). Three diagonal lines representing the lithology types such as dolomite, calcite (limestone), and quartz are plotted in this cross plot (Fig. 5); this method is called the indirect method for determining lithology because no rock samples are used (Priisholm and Michelsen, 1979).

According to Bowler (1981), if a point falls on the calcite (limestone) diagonal line, it indicates that the rock consists predominantly of limestone. On the other hand, if a point falls between the limestone (calcite) and dolostone (dolomite) lines, it suggests that the rock is a combination of limestone and dolostone known as dolomitic limestone.

The N-D cross-plot chart (Fig. 5) indicates that the lithology is predominantly composed of dolomite and dolomitic limestone because the greatest number of plotted points fall along the dolomite line and the line between dolomite and limestone, and there is also an amount of limestone and little marl because some points fall along the limestone and sandstone line. This indicates that the successions of the Sinjar Formation include mainly dominant dolomite and dolomitic limestone (upper unit) with some interbeds of dolomitic limestone and limestone (lower unit).
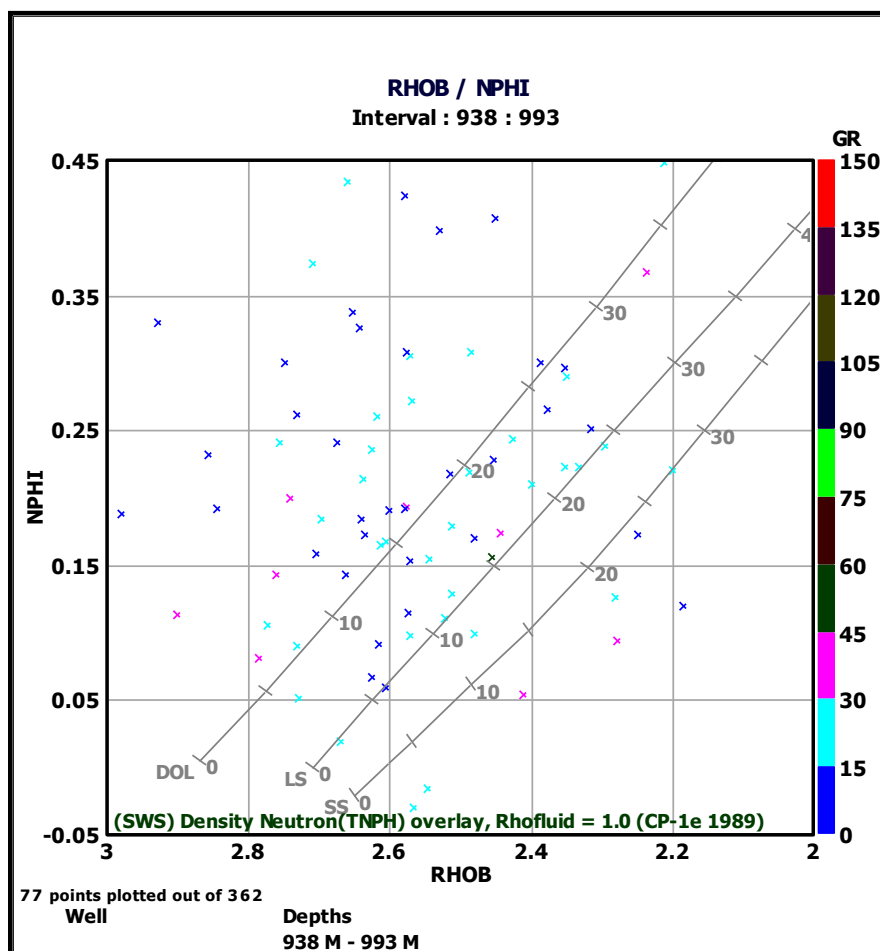
Fig. 5. Lithology Determination of the studied formation from the N-D cross plot.

4- Porosity (ɸ) calculation

The porosity is defined as the ratio of the total pore space in the rock to that of the bulk volume. Porosity is an important rock characteristic that reflects the fluid storage capacity and its evaluation in the reservoir and is measured by well logging (Tiab and Donaldson, 2015). It

is an inexpensive and rapid technique for obtaining accurate information and its identification is through petrographic study.

The porosity and permeability of carbonate rocks are influenced by various factors such as texture, grain size, and grain arrangement as well as diagenetic processes (dolomitization, fracturing, and dissolution), which are very significant because they can create effective secondary porosity (Choquette and Pray, 1970). The pores in the rocks must be interconnected, thereby allowing fluids mobility within the reservoir and thence flow to a production well (Speight, 2017). Porosity is calculated as follows:

A- Compensated Neutron Log (CNL):

CNL directly measures the porosity of the formation's rocks. The recorded values represent neutron porosity (ϕN). Neutron porosity is typically a fraction or percentage (Fig. 6).

B- Formation Density Compensated (FDC):

According to Ezekwe (2010), FDC has a radioactive source equipped with two detectors, and indirectly measures the porosity of the formation's rocks by measuring total porosity from the formation density compensated (ϕD) and fluid density ($\rho fluid$) (Fig. 6) of the fluid that fills the pores given in grams per cubic centimeter (g/cm³). It is calculated according to the following equation (3).

$$\phi_D = (\rho_{max} - \rho_b) / (\rho_{max} - \rho_{fluid}) \ldots\ldots\ldots\ldots (3)$$

where: ϕ_D = Porosity from density log; ρ_b = Formation bulk density in g/cm³; ρ_{max} = The density of rock matrix in g/cm³; ρ_{fluid} = The density of fluid occupying pore spaces (0.74 g/cm³ for gas, 0.9 g/cm³ for oil, 1.0 g/cm³ for freshwater, and 1.1 g/cm³ for saltwater mud).
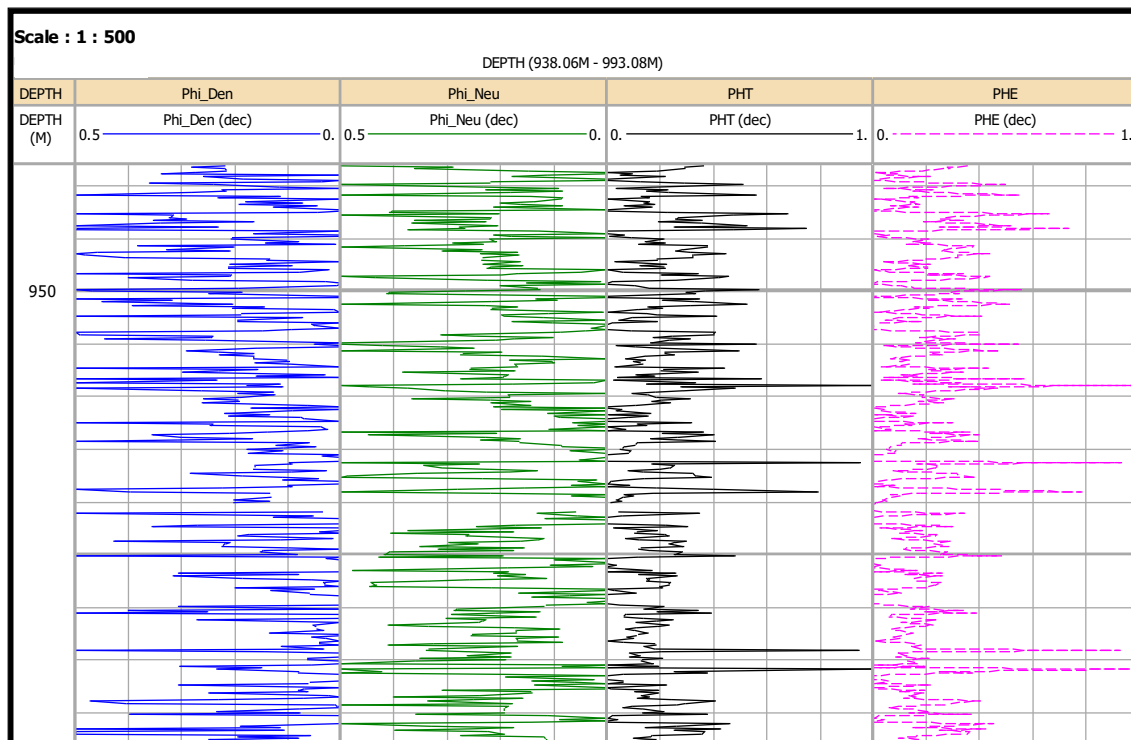
Fig. 6. Porosity logs including neutron, density, neutron-density logs data, and effective porosity for the studied formation.

C- Combination of Neutron-Density Porosity Logs (Φ_{N-D})

According to Schlumberger (1974), the association of neutron and density measurements is the most reliable and representative at any depth for estimating average neutron and density porosity (ϕ_{N-D}). This association is called total porosity (ϕ_T), which is the total amount of voids

in the rock volume and is calculated using equation (4). Figure (5) shows that the density porosity is greater than the neutron porosity except in some intervals this effect is not observed due to the predominance of dolomite.

$$\phi_{N\text{-}D} = (\phi_N + \phi_D) / 2 \dots\dots\dots\dots\dots (4)$$

where: $\phi_{N\text{-}D}$= Total porosity derived from the neutron and density logs; ϕ_N= Porosity derived from neutron log; ϕ_D= Porosity derived from density log.

D- Effective porosity (ϕ_E)

It is the ratio of the volume of interconnected pores available for fluids to the total volume of the rock. It can be calculated by equation (5) after correcting the total porosity from the shale volume (Schlumberger, 1989).

$$\phi_E = \phi_T * (1\text{-}V_{Sh}) \dots\dots\dots\dots (5)$$

where: ϕ_E= Effective porosity; ϕ_T= Total porosity derived from neutron and density logs; V_{Sh}= Volume of shale.

To evaluate average porosity from density and neutron logs, figure (6) shows the distribution of total porosity with effective porosity along the length of the studied well. Based on the porosity values calculated by Schlumberger (1974), the log curve is divided into two different porosity units.

In the upper unit, the minimum and maximum porosity values are recognized for the density log range from 0.06 to 0.47, and in the neutron log, the range is from 0.05 to 0.45. Additionally, in the lower unit, the minimum and maximum porosity values are recognized for the density log range from 0.04 to 0.4, and in the neutron log, the range is from 0.03 to 0.35.

Depending on this information, the reservoir units within the Sinjar Formation show that the porosity in its upper part is greater than that in the lower part due to the predominance of dolomite.

5- Porosity classification

The porosity of the formation is classified according to the system proposed by Lucia (1995), which divides the porosity into two main types: interparticle porosity (Fig. 7) and intraparticle porosity (Fig. 8). The classification utilizes petrophysical-textural terms to describe the porosity characteristics observed in the formation, whether these pores are of sedimentary or diagenetic origin. Below is a description of the porosity types and how common they are within the formation sequences.
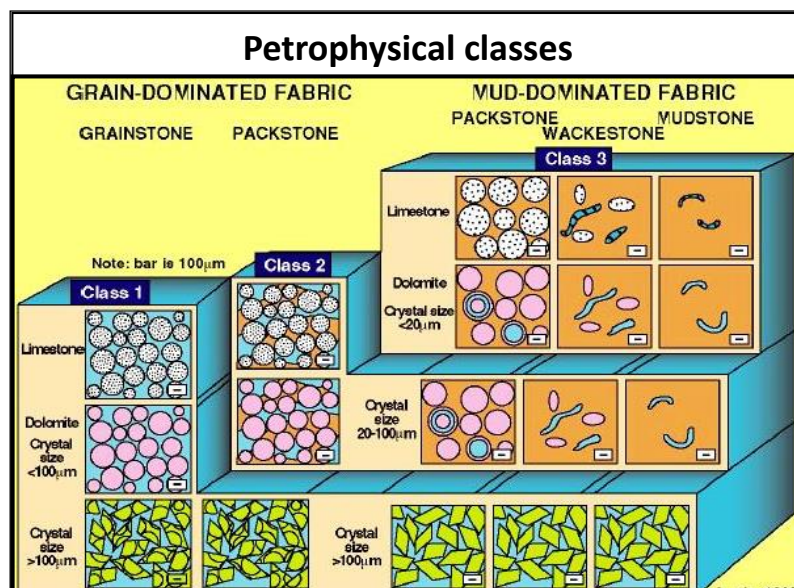

Fig. 7. Petrophysical classification of interparticle porosity (Lucia, 1995).
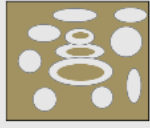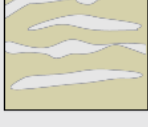
Fig. 8. Petrophysical classification of intraparticle porosity (Lucia, 1995).

1- Interparticle or intercrystalline porosity

This type of porosity refers to the pore space of intergrain or intercrystal within rocks, and this porosity has various forms after dissolving minerals or removing fossils. The classification of Lucia (1995) depends mainly on the size and sorting of grains, which play an important role in determining the amount and connectivity of the pore spaces. Therefore, Lucia (1995) classified the interparticle porosity into three classes (a, b, c) based on Dunham **classification** (1962) whether the texture is mud-supported or grain-supported as exhibited in Figure (7).

Class a: The interparticle porosity is represented by grain-supported (grainstone) facies and is characterized by coarse sorted grains resulting in high porosity (Fig. 9-A). This class is useful for improving the constancy of the formation and its pressure resistance (Lucia, 1995)

Class b: The interparticle porosity is represented by grain-supported (packstone) facies and is characterized by moderately sized and sorted grains resulting in moderate porosity (Fig. 9-B). This class is considered the most important in expressing its hydrocarbon content in the formation sequences as the bituminous materials spread in it within the dolomite crystals and help fluids to distribute within the formation.

Class c: The interparticle porosity is represented by mud-supported (mudstone) facies and is characterized by small and poorly sorted grains resulting in low porosity compared to grainstone and packstone facies (Fig. 9-C).
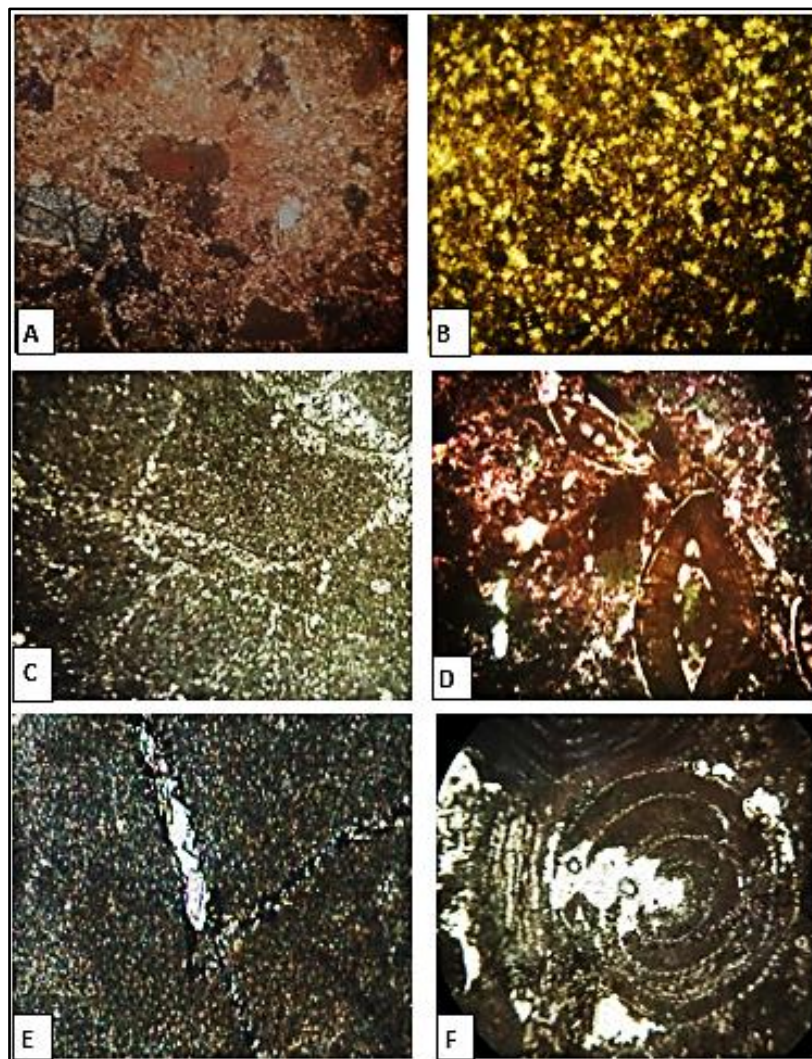
Fig. 9. Different types of pores identified in Sinjar Formation. 1. Intergrain porosity: (A) Coarse grains, (B) Medium grains, (C) Fine grains. 2. Vuggy porosity: (D) Separate vug pores, (E) Fractional pores, (F) Touching vug pores.

2- Vuggy Porosity (Intraparticle) porosity

This kind of porosity refers to the pores found within the intraparticles or intrarcrystals in rocks and can take various forms such as dissolved granules, fractures, or irregularly shaped caves. According to the classification of Lucia (1995), the vuggy porosity can be classified into two types according to the nature of their connection to each other (Fig. 8) as follows:

Separate vug pores: They are isolated pores connected through interparticle pores. Although these pores can increase the total porosity of the rock, they have limited reservoir importance (Lucia, 1995). However, in certain cases, such as in supportive clay rocks, these pores can form an effective and important reservoir of porosity (Moore, 1979). The current research has identified the occurrence of separate vug pores within the fossils of the studied formation (Fig. 9-D).

Touching vug pores: They are characterized by their larger sizes compared to the surrounding granules or crystals with a predominance of fractional pores (Fig. 9-E) and vuggy pores (Fig. 9-F). These pores form an interconnected pore system resulting in enhanced porosity for the reservoir potential within the studied formation sequences.

6- Reservoir partitioning

Based on the calculated porosity values, Sinjar Formation can be divided into two parts (upper and lower) (Fig. 10).

Upper part

It has a thickness of approximately (32 m) between depths of (938 and 970 m). It consists of yellowish-gray dolomitic limestone, and is divided into two zones (A and B):

Zone A: This zone is located between depths of (938 and 959m) and has a thickness of about (21 m). The porosity of this zone is described as very good (25-35%), making it known as a perfect reservoir rock according to explorational geology literature.

Zone B: This zone is located between depths of (959 and 970 m) and has a thickness of about 11 m). The porosity of this zone is described as intermediate-good (10-25%), making it known as intermediate-good reservoir rocks according to explorational geology literature.

Lower part

Its thickness is approximately (23 m); that is, between the depths (970 and 993m). It consists of white limestone and dolomitic limestone, and is divided into two zones (C and D):

Zone C: This zone is located between depths of (970 and 985 m) and has a thickness of about (15 m). The porosity of this zone is described as poor (5-12%) making it known as poor reservoir rocks according to explorational geology literature.

Zone D: This zone is located between depths of (985 and 993 m) and has a thickness of about 8 meters. The porosity of this zone is described as intermediate-good (10-25%) making it known as intermediate-good reservoir rocks according to explorational geology literature.
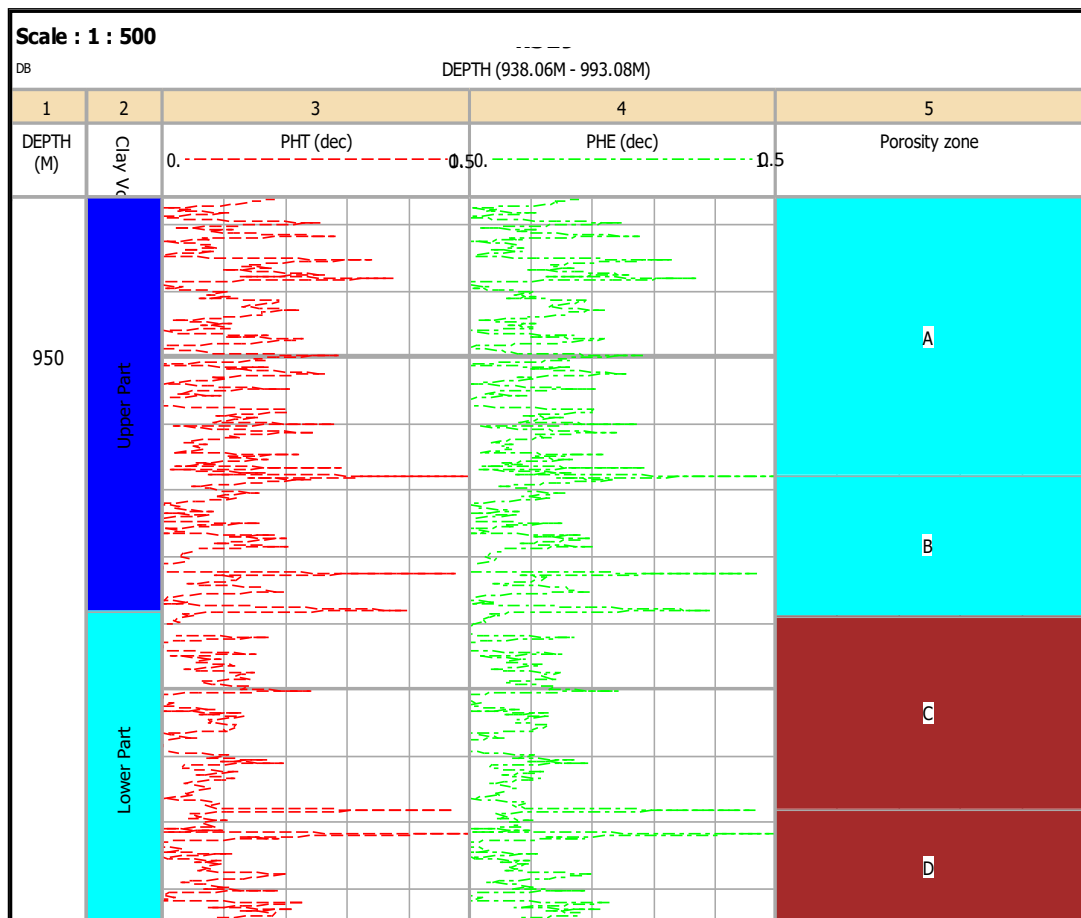

Fig.10. The reservoir partitioning of the Sinjar Formation.

Based on this information, the porosity values indicate that the effective porosity (Φ) is low in zone C, moderate to good in zones B and D, and very good in zone A (Fig. 10). In general, these values indicate that the upper part of the Sinjar Formation has a higher porosity compared to the lower part due to the predominance of dolomite.

Conclusion

Based on the evaluation of the reservoir potential of the Sinjar Formation (Paleocene-Early Eocene) using well logs data and cutting samples from well (K-319) in the Kirkuk Oilfield in northeastern Iraq, the following inferences can be drawn:

The lithology description of the Sinjar Formation indicates the dominance of limestone and dolomitic limestone in the lower part, with a dominance of dolomitic limestone in the upper part. The presence of shale less than (10%) within the Sinjar Formation reduced the effective porosity and affected the reservoir quality.

Two main porosity types are identified in the studied successions, intergrain and vuggy porosity. Interparticle porosity is divided into three classes: Class A (grainstone facie), Class B (packstone facies), and Class C (mudstone facies). On the other hand, vuggy porosity can be divided into two types based on the nature of its interconnection with each other: separate vug pores, and touching vug pores. Vuggy porosity can significantly enhance the overall porosity of the formation, allowing for improved fluid flow and storage capacity.

The petrophysical characteristics are determined through reservoir rocks subdivision into four porosity zones in the Sinjar Formation. The Reservoir Zone C has poor porosity ranging from (5%-12%), zones B and D have intermediate to good porosity ranging from (10%-25%), and zone A has very good porosity ranging from (25%-35%).

Overall, the petrophysical properties and geological features identified in this study indicate that the carbonate reservoir has intermediate-good potential; additionally, the upper part of the formation in general has higher porosity compared to the lower part as a result of the dolomite predominance and the presence of fractures and vugs; this indicates that the upper part of the formation may have better fluid flow and storage capabilities making it more favorable target for potential hydrocarbon exploration and production.

Acknowledgements

References

Alatroshe, R.K. H., Algburi A.R. and Ahmed F.M., 2023. Diagenetic processes of Shiranish Formation in Bekhair Anticline, Duhok Governorate, Iraqi National Journal of Earth Sciences, Vol. 23, No. 1, pp. 26-50. DOI:10.33899/EARTH.2022.134982.1021

Al-Saddiki, A., 1968. Stratigraphy and microfacies from Sinjar Formation. Unpub. M.Sc. Thesis, University of Baghdad. 208 p.

Al-Sakini, J, A., 1992. Al-Wajeez in the Petroleum Geology of Iraq and the Middle East. Internal Report in Arabic, Northern Petroleum Company, Kirkuk. 179 p.

Aqrawi, A. A. M., 1998. Paleozoic Stratigraphy and Petroleum Systems of the Western and Southwestern Deserts of Iraq. Geo Arabia, Vol. 3, No.2, pp. 229-248. DOI: 10.2113/geoarabia0302229

Aqrawi, A. A. M., Horbury, A.D., Goff, J.C. and Sadooni, F.N., 2010. The Petroleum Geology of Iraq. Beacons Field, Bucks, UK: Scientific Press Ltd, Great Britain, 424 p.

Asquith, G., Krygowski, D., 2004. Basic well log analysis. Vol. 16, American Association of Petroleum Geologists, Tulsa, pp. 31-34. DOI: https://doi.org/10.1306/Mth16823.

Assaad, F. A., 2009. Field methods for petroleum geologists: A guide to computerized lithostratigraphic correlation charts case study: Northern Africa. Springer, 133 p.

Bassiouni, Z., 1994. Theory Measurement and Interpretation of Well Logs. Richardson, TX: Henry L. Doherty Memorial Fund of AIME, Society of Petroleum Engineers.

Bellen, R. C. V., Dunnington, H. V., Wetzel, R. and Morton, D., 1959. Lexique Stratigraphique International Asie, Iraq. Vol. 3C, No.10a, 333 p. DOI: https://api.semanticscholar.org/CorpusID:128726684

Bhuyan, K. and Passey, Q. R., 1994. Clay Estimation from Gr and Neutron -Density Porosity Logs. Paper presented at the SPWLA 35th Annual Logging Symposium, Tulsa, Oklahoma.

Bowler, J. 1981. The litho-density log. The APPEA Journal, Vol.21, No.1, pp. 200-212.

Burke, J. A., Campbell, R. L., Jr. and Schmidt, A. W., 1969. The litho-porosity cross plot: A method of determining rock characteristics for computation of log data. SPE Illinois Basin Regional Meeting, Evansville, Indiana, Paper Number: SPE-2771-MS, DOI: https://doi.org/10.2118/2771-MS

Choquette, P. W. and Pray, L. C., 1970. Geologic Nomenclature and Classification of Porosity in Sedimentary Carbonates. AAPG. Bull., Vol. 54, No.2, pp. 207-250. DOI: https://doi.org/10.1306/5D25C98B-16C1-11D7-8645000102C1865D.

Dunham, R. J., 1962. Classification of Carbonate Rocks According to Depositional Texture. In: Ham, W.E., Ed., Classification of Carbonate Rocks, AAPG, Tulsa, pp.108-121.

Ezekwe, N., 2010. Petroleum Reservoir Engineering Practice. Upper Saddle River, NJ: Prentice-Hall.

Fadhil, D. T., Theyab. M. A. and Al-Hadidy. A. 2021, Petrographical and microfacies study of Sinjar Formation in Bazyan anticline, Sulaymaniyah region (Northern Iraq), Naukovyi Visnyk Natsionalnoho Hirnychoho Universytetu, No. 6, pp. 11-15. DOI: https://doi.org/10.33271/nvngu/2021-6/011

Fouad, S. F. A., 2015. Tectonic Map of Iraq. scale 1: 1000000, 3rd Edition, Iraqi Bulletin of Geology and Mining, Iraq, Vol. 11, No.1, pp. 1-7. DOI: https://ibgm-iq.org/ibgm/index.php/ibgm/article/view/262.

Garland, C. R., Abalioglu, I., Akca, L., Cassidy, A., Chiffoleau, Y., Godail, L., Grace, M. A. S., Kader, H. J., Khalek, F., Legarre, H., Nazhat, H. B. and Sallier, B., 2010. Appraisal and development of the Taq Taq field, Kurdistan region, Iraq. Geological Society, London, Petroleum Geology Conference series, Vol. 7, pp. 801-810. DOI: https://doi.org/10.1144/0070801.

Ghorab, M., Mohamed, A. M. R. and Nouh, A. Z., 2008. The relation between the shale origin (source or non-source) and its type for Abu Roash Formation at Wadi El-Natrun Area, South of Western Desert, Egypt. Australian Journal of Basic and Applied Sciences, Vol. 2, No.3, pp. 360-371.

Hussein, D., Lawrence. J. Rashid, F., Glover, P. and Lorinczi, P., 2018. Developing pore size distribution models in heterogeneous carbonates using, especially nuclear magnetic resonance. Engineering in Chalk, ICE publishing ISBN 978-0-7277-6407-2. pp. 529-534. DOI: https://doi.org/10.1680/eiccf.64072.529.

Hussein, D. O., 2021. Evaluation of reservoir potentiality of the Sinjar Formation within the Taq-Taq Oilfield, Kurdistan region, Iraq. Iraqi Bulletin of Geology and Mining. Vol. 17, No.1, pp. 73-85.

Jassim, S. Z. and Goff, J. C., 2006. Geology of Iraq. Published by Doline, Prague and Moravian Museum, Brno, Czech Republic, 341 p.

Karim., K. H., Daoud., H. S. and Kuradawy., A. R. H., 2018. Record of Khurmala Formation (Late Paleocene – Early Eocene) in the Sulaymaniyah Governorate, Kurdistan Region, Northeast Iraq. Iraqi Geological Journal, Vol. 51, No.1, pp. 34-55. DOI: https://doi.org/10.46717/igj.51.1.3Ms-2018-06-25.

Larionov, V. V., 1969. Borehole Radiometry: Moscow, U.S.S.R., Nedra. 112P in Asquith, G. and Krygowski, D., 2004. Basic Well Log Analysis. AAPG Methods in Exploration Series, Vol. 16, 204 p.

Lucia, F.J., 1995. Rock Fabric/Petrophysical classification of carbonate pore space for reservoir characterization. AAPG Bulletin, Vol. 79, No.9, pp. 1275-1300.

Moore, C. H., 1979. Porosity in Carbonate Rock Sequence. In: Moore, C.H., (eds.), Geology of Carbonate Porosity. Course Note Series 11, AAPG. Continuing Education: A1-A124,

North Oil Company, 1990. Final Report of the Kirkuk Well (K-319), Geological Department, North Oil Fields Authority, Kirkuk, unpublished report.

Paul, G., 2010. Introduction to petrophysics and formation evaluation. Petrophysics. MSc Course Notes. pp. 1-9.

Priisholm, S. and Michelsen, O. 1979. The use of porosity logs in lithology determination, lithostratigraphy and basin analysis. Geomathematical and Petrophysical Studies in Sedimentology: An International Symposium, Elsevier. Pergamon Press Ltd. Published by Elsevier Ltd., pp. 71-79.

Rashid, F., Glover, P. W. J., Lorinczi, P., Hussein, D. and Lawrence, J. A., 2017. Microstructural controls on reservoir quality in tight oil carbonate reservoir rocks. Journal of Petroleum Science and Engineering, Vol. 156, pp. 814-826. DOI: https://doi.org/10.1016/j.petrol.2017.06.056.

Rashid, F., Hussein, D. O. and Zangana, H. A., 2020. Petrophysical Investigation of the Khurmala Formation in Taq Taq Oil Field, Zagros Folded Belt. The Scientific Journal of Koya University. Vol. 8, No.1. DOI: https://doi.org/10.14500/aro.10556 .

Rider, M. H. and Kenedy, M., 2011. The Geological Interpretation of Well Logs, Sutherland, Rider-French Consulting Ltd, 432 p.

Schlumberger, 1974. Log Interpretation. Vol. 2 –Application. by Schlumberger, USA., 116 p.

Schlumberger, 1989. Cased Hole Log Interpretation Principles/Applications, Houston, Schlumberger Wireline and Testing.

Schlumberger, 1997. Log Interpretation Charts. Houston, USA, Schlumberger Wireline and Testing.

Speight, J., G., 2017. Deep Shale Oil and Gas. Gulf Professional Publishing is an imprint of Elsevier. 481 p.

Tiab, D., Donaldson, E.C., 2015. Petrophysics: Theory and Practice of Measuring Reservoir Rock and Fluid Transport Properties: Fourth Edition, Gulf Professional Publishing is an imprint of Elsevier. DOI: https://doi.org/10.1016/C2014-0-03707-0.